

# Extrapolating the thermodynamic length with finite-time measurements

Jin-Fu Chen,<sup>1,2</sup> C. P. Sun,<sup>1,2,\*</sup> and Hui Dong<sup>2,†</sup>

<sup>1</sup>Beijing Computational Science Research Center, Beijing 100193, China

<sup>2</sup>Graduate School of China Academy of Engineering Physics,

No. 10 Xibeiwang East Road, Haidian District, Beijing, 100193, China

(Dated: June 19, 2021)

The excess work performed in a heat-engine process with given finite operation time  $\tau$  is bounded by the thermodynamic length, which measures the distance during the relaxation along a path in the space of the thermodynamic state. Unfortunately, the thermodynamic length, as a guidance for the heat engine optimization, is beyond the experimental measurement. We propose to measure the thermodynamic length  $\mathcal{L}$  through the extrapolation of finite-time measurements  $\mathcal{L}(\tau) = \int_0^\tau [P_{\text{ex}}(t)]^{1/2} dt$  via the excess power  $P_{\text{ex}}(t)$ . The current proposal allows to measure the thermodynamic length for a single control parameter without requiring extra effort to find the optimal control scheme. We illustrate the measurement strategy via examples of the quantum harmonic oscillator with tuning frequency and the classical ideal gas with changing volume.

*Introduction.*—Optimization of thermodynamic processes is of practical importance in finite-time thermodynamics [1–6] to minimize the dissipation in finite-time transformation processes [7–11], and to improve the performance of real heat engines [12–20]. The extent, to which the optimization can be achieved, is discovered to be limited by the geometry properties of the thermodynamic equilibrium state space [21–27] and provides a criterion for the amelioration of specific control schemes. For a finite-time isothermal process with operation time  $\tau$ , such optimization is realized by minimizing the entropy production [28–31] or the excess work  $W_{\text{ex}} = W - \Delta F$  [32–34], where  $W$  is the total performed work and  $\Delta F$  is the free energy change. For a given control scheme, the excess work at the long-time limit is bounded as  $W_{\text{ex}} \geq \mathcal{L}^2/\tau$  [35–40], where  $\mathcal{L}$  is the thermodynamic length during the relaxation dynamics [41–44]. In the recent development of finite-time quantum thermodynamics [45–49], the thermodynamic length relates to the geometric measures of quantum states, such as the Bures length and the Fisher or the Wigner-Yanase skew information [50–54], and provides a lower bound of the excess work and the entropy production in a finite-time quantum thermodynamic process [55–58].

However, it remains a challenge to practically measure the thermodynamics length in a real thermodynamic system. To obtain the metric of the state space, one needs the exact equilibrium thermal states along the path of the control parameters, which could be the frequency of harmonic oscillator or the volume of the classical ideal gas. One proposal for the measurement is the utilization of the discrete-step process [26, 27], which requires significant amount of small steps. In this Letter, we define a finite-time thermodynamic length  $\mathcal{L}(\tau)$ , which retains the thermodynamic length at the long-time limit. The thermodynamic length  $\mathcal{L}$  can be measured through extrapolating few data points of  $\mathcal{L}(\tau)$  with finite duration  $\tau$ . The measurement procedure is illustrated via examples of the quantum harmonic oscillator with tuning frequency

and the classical ideal gas with changing volume.

*Finite-time thermodynamic length.*—We consider an open quantum system with the control parameter  $\lambda(t)$  tuned from the initial value  $\lambda(0) = \lambda_0$  to the final value  $\lambda(\tau) = \lambda_\tau$  in a finite-time process with duration  $\tau$ . The system state is described by the density matrix  $\rho(t)$  ( $0 < t < \tau$ ), which evolves under the time-dependent Hamiltonian  $H(t) = H[\lambda(t)]$  via the time-dependent Markovian master equation [59–61]

$$\dot{\rho} = \mathcal{L}_{\lambda(t)}\rho, \quad (1)$$

where  $\mathcal{L}_{\lambda(t)}$  is the quantum Liouvillian super-operator. In quantum thermodynamics, the rate of the performed work, namely the power, is  $\dot{W} = \text{Tr}(\rho\dot{H})$  [62]. In a quasi-static isothermal process with infinite duration, the system evolves along the trajectory of the equilibrium state  $\rho_{\text{eq}}(t) = \exp[-\beta_{\text{b}}H(t)]/\text{Tr}\{\exp[-\beta_{\text{b}}H(t)]\}$  with the inverse temperature  $\beta_{\text{b}} = 1/k_{\text{B}}T_{\text{b}}$  of the bath, and the performed work of the whole process is  $W_{(0)} = \int_{\lambda_0}^{\lambda_\tau} \text{Tr}(\rho_{\text{eq}}\partial H/\partial\lambda)d\lambda$ . In a finite-time isothermal process, the excess work  $W_{\text{ex}}(\tau) = \int_0^\tau P_{\text{ex}}(t)dt$  is utilized to evaluate the dissipation with the excess power [41]  $P_{\text{ex}}(t) = \dot{W}(t) - \dot{W}_{(0)}(t)$ , where  $\dot{W}_{(0)}(t) = \text{Tr}[\rho_{\text{eq}}\dot{H}]$  is the quasi-static part of the work rate. One important progress [41, 42] for the finite-time thermodynamics is the discovery of the geometric bound of the excess work with the thermodynamic length as  $W_{\text{ex}}(\tau) \geq \mathcal{L}^2/\tau$ , and the equality is saturated by the optimal protocol with the constant excess power. The direct measurement of thermodynamic length  $\mathcal{L}$  requires the infinite slow isothermal processes [26, 27].

In quantum thermodynamics, the thermodynamic length  $\mathcal{L}$  is explicitly [55]

$$\mathcal{L} = \int_{\lambda_0}^{\lambda_\tau} \sqrt{\text{Tr}\left[\frac{\partial H}{\partial\lambda} \mathcal{L}_\lambda^{-1}\left(\frac{\partial\rho_{\text{eq}}}{\partial\lambda}\right)\right]}d\lambda, \quad (2)$$

which contains the Drazin inverse  $\mathcal{L}_\lambda^{-1}$  of the super-operator [63, 64]. For the diagonalizable super-operator,

the Drazin inverse is explicitly obtained as follows. The eigendecomposition is  $\mathcal{L}_\lambda = \sum_\Gamma \Gamma P_\Gamma$  with the eigenvalues  $\Gamma$  and the projections  $P_\Gamma$  in the super-space of the density matrices. The null eigenvector is the instantaneous equilibrium state satisfied  $\mathcal{L}_\lambda[\rho_{\text{eq}}(\lambda)] = 0$ . The Drazin inverse is then written as  $\mathcal{L}_\lambda^{-1} = \sum_{\Gamma \neq 0} \Gamma^{-1} P_\Gamma$ , where the inverses of the non-zero eigenvalues  $\Gamma^{-1}$  determines different dissipation timescales [63, 64]. Detailed discussions about the Drazin inverse are given with an example of the two-level system in the Supplementary Materials [65].

For the measurement, we define a finite-time thermodynamic length as

$$\mathcal{L}(\tau) = \int_0^\tau \sqrt{P_{\text{ex}}(t)} dt. \quad (3)$$

The two following properties of the finite-time thermodynamic length allows the measurement of the thermodynamic length with the extrapolation of finite-time measurements.

(i) **The convergence**  $\lim_{\tau \rightarrow \infty} \mathcal{L}(\tau) = \mathcal{L}$ . In a slow isothermal process, the state of the system evolves near the equilibrium state, and the solution to Eq. (1) is expanded in the series [39] as

$$\rho(t) = \sum_{n=0}^{\infty} \left( \mathcal{L}_{\lambda(t)}^{-1} \frac{d}{dt} \right)^n \rho_{\text{eq}}(t). \quad (4)$$

For a given tuning protocol  $\lambda(t) = \tilde{\lambda}(t/\tau)$ , the series expansion of the excess power is obtained as

$$P_{\text{ex}}(t) = \text{Tr} \left\{ \frac{\partial \tilde{H}(s)}{\partial s} \sum_{n=1}^{\infty} \tau^{1-n} \left( \mathcal{L}_{\tilde{\lambda}(s)}^{-1} \frac{\partial}{\partial s} \right)^n [\tilde{\rho}_{\text{eq}}(s)] \right\}, \quad (5)$$

where  $s = t/\tau$  is the rescaled dimensionless time. Equation (5) is invalid at the beginning of the isothermal process. Its validity requires a relaxation with the time larger than the typical dissipation timescale. For the slow process, the lowest-order term with  $n = 1$  dominates the summation, and the finite-time thermodynamic length approaches the thermodynamic length at the long-time limit.

(ii) **The protocol independence of the limit**  $\lim_{\tau \rightarrow \infty} \mathcal{L}(\tau)$ . For the system with only one control parameter, the limit of the finite-time thermodynamic length  $\lim_{\tau \rightarrow \infty} \mathcal{L}(\tau)$  is independent of the protocol, which implies the thermodynamic length can be measured without necessarily using the optimal protocol. For multiple control parameters, the limit  $\lim_{\tau \rightarrow \infty} \mathcal{L}(\tau)$  indeed relies on the path of the protocol. The minimal thermodynamic length is only reached by the geodesic path, and the optimized protocol is to tune the control parameter with the constant velocity of the thermodynamic length [55].

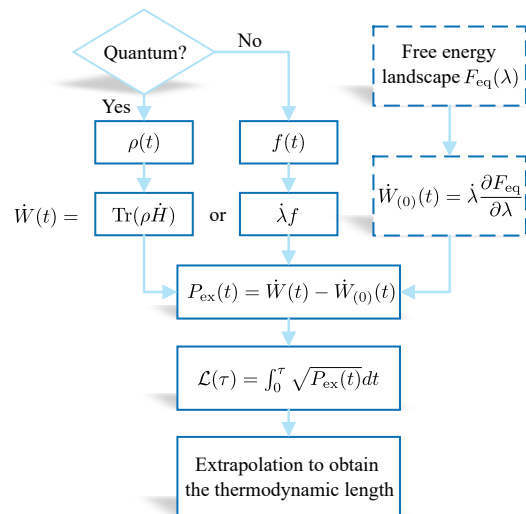


Figure 1. (Color online) Flowchart for measuring the thermodynamic length  $\mathcal{L}$  with finite-time extrapolation. The excess power is evaluated with the performed work rate  $\dot{W}(t)$  and the quasi-static work rate  $\dot{W}_{(0)}(t)$  at each moment of the finite-time process.

*Measurement strategy.*—The thermodynamic length is the long-time limit of the finite-time thermodynamic length. In the following, we propose an extrapolation method to measure the thermodynamic length for the system with a single control parameter. The flowchart of the method is shown in Fig. 1. The measurement of the finite-time thermodynamic length  $\mathcal{L}(\tau)$  requires the excess power  $P_{\text{ex}}(t)$  of the whole process. The power  $\dot{W}(t)$  ( $0 < t < \tau$ ) in a finite-time process is measured through the conjugate force  $f(t) = \text{Tr}[\rho \partial_\lambda H]$  for a classical system via  $\dot{W}(t) = \dot{\lambda}(t) f(t)$  or the tomography of the density matrix  $\rho(t)$  for a quantum system via  $\dot{W}(t) = \text{Tr}(\rho \dot{H})$ . With the given protocol  $\dot{\lambda}(s)$  of the control parameter, the quasi-static work rate  $\dot{W}_{(0)}(t) = \text{Tr}(\rho_{\text{eq}} \dot{H}) = \dot{\lambda} \partial_\lambda F_{\text{eq}}(\lambda)$  is obtained with the landscape of the equilibrium free energy  $F_{\text{eq}}(\lambda)$ , which can be typically obtained from finite-time processes via Jarzynski's equality [66].

Assuming the length  $\mathcal{L}(\tau)$  as a smooth function of the duration  $\tau$ , we expand  $\mathcal{L}(\tau)$  with the Laurent series as

$$\mathcal{L}(\tau) = \mathcal{L} + \sum_{j=1}^{\infty} \frac{a_j}{\tau^j}. \quad (6)$$

The duration  $\tau$  needs to be chosen notably larger than the dissipation timescale to ensure the validity of Eq. (5). By measuring the finite-time thermodynamic length under given duration, we extrapolate the function as  $\mathcal{L}(\tau) = \mathcal{L} + \sum_{j=1}^N a_j \tau^{-j}$  with the cutoff  $N$ . The thermodynamic length  $\mathcal{L}$  is estimated with the extrapolation  $\tau \rightarrow \infty$ . We apply the current strategy to measure the thermodynamic length with two examples, i.e. the quan-

tum harmonic oscillator and the classical ideal gas system.

*Quantum harmonic oscillator with tuned frequency.*— We consider the quantum Brownian motion with the Hamiltonian  $H(t) = \hat{p}^2/(2m) + m\omega(t)^2\hat{x}^2/2$  in a tuned harmonic potential with the frequency  $\omega(t)$  as the control parameter in the finite-time isothermal process. At the high temperature limit, the evolution of the reduced system is described by the Caldeira-Leggett master equation [67, 68], i.e.,  $\partial_t\rho = \mathcal{L}_{\omega(t)}\rho$ . The quantum Liouvillian super-operator is explicitly

$$\mathcal{L}_{\omega(t)}\rho = -i[H(t), \rho] - i\kappa[\hat{x}, \{\hat{p}, \rho\}] - \frac{2m\kappa}{\beta_b}[\hat{x}, [\hat{x}, \rho]], \quad (7)$$

$$\frac{d}{dt} \begin{pmatrix} \langle H \rangle \\ \langle L \rangle \\ \langle D \rangle \end{pmatrix} = \begin{pmatrix} -2\kappa + \frac{\dot{\omega}}{\omega} & -2\kappa - \frac{\dot{\omega}}{\omega} & 0 \\ -2\kappa - \frac{\dot{\omega}}{\omega} & -2\kappa + \frac{\dot{\omega}}{\omega} & -2\omega \\ 0 & 2\omega & -2\kappa + \frac{\dot{\omega}}{\omega} \end{pmatrix} \begin{pmatrix} \langle H \rangle \\ \langle L \rangle \\ \langle D \rangle \end{pmatrix} + 2\kappa k_B T_b \begin{pmatrix} 1 \\ 1 \\ 0 \end{pmatrix}. \quad (8)$$

The derivation to Eqs. (8) is presented in the Supplementary Materials [65].

The performed work rate of the tuned harmonic oscillator is  $\dot{W} = \dot{\omega}/\omega (\langle H \rangle - \langle L \rangle)$ . In a quasi-static isothermal process, the system evolves along the equilibrium states with the average internal energy  $\langle H \rangle = k_B T_b$  and the average Lagrange  $\langle L \rangle = 0$ , and the quasi-static work rate is  $\dot{W}_{(0)}(t) = k_B T_b \dot{\omega}/\omega$ . In a finite-time process, the finite-time thermodynamic length  $\mathcal{L}(\tau)$  is explicitly

$$\mathcal{L}(\tau) = \int_0^\tau [\dot{\omega}/\omega (\langle H \rangle - \langle L \rangle - k_B T_b)]^{1/2} dt. \quad (9)$$

The thermodynamic length of the tuned harmonic oscillator is obtained by Eq. (2) as

$$\mathcal{L} = \sqrt{\frac{k_B T_b}{2\kappa}} \left| \left[ \sinh^{-1}\left(\frac{\omega}{2\kappa}\right) - \sqrt{1 + \frac{4\kappa^2}{\omega^2}} \right] \Big|_{\omega=\omega_0}^{\omega_\tau} \right|, \quad (10)$$

where  $\omega_0$  and  $\omega_\tau$  are the initial and final frequencies of the harmonic potential. The detailed derivation of the thermodynamic length is given in the Supplementary Materials [65]. The optimal protocol  $\omega_{\text{op}}(t) = \tilde{\omega}_{\text{op}}(t/\tau)$  satisfies

$$\left( \frac{1}{2\kappa} + \frac{2\kappa}{\tilde{\omega}_{\text{op}}^2} \right)^{1/2} \frac{1}{\tilde{\omega}_{\text{op}}} \frac{d\tilde{\omega}_{\text{op}}(s)}{ds} = \text{const.} \quad (11)$$

For small damping rate  $\kappa \ll \omega$ , the thermodynamic length approximates  $\mathcal{L} \approx \sqrt{k_B T_b/(2\kappa)} |\ln \omega_\tau/\omega_0|$ , and the optimal protocol is the exponential protocol  $\tilde{\omega}_{\text{op}}(s) = \omega_0 \exp[s \ln(\omega_\tau/\omega_0)]$ . For the large damping rate  $\omega \ll \kappa$ , the thermodynamic length approximates  $\mathcal{L} \approx \sqrt{2\kappa k_B T_b} |(\omega_\tau - \omega_0)/(\omega_0 \omega_\tau)|$ , and the optimal protocol is the inverse protocol  $\tilde{\omega}_{\text{op}}(s) = \omega_0 \omega_\tau / [(\omega_0 - \omega_\tau)s + \omega_\tau]$ .

where the frequency-independent damping rate  $\kappa$  is induced by the Ohmic spectral of the heat bath [67, 68].

With the infinite dimension of the Hilbert space for a harmonic oscillator, it is difficult to solve the evolution of the density matrix by calculating the Drazin inverse of the super-operator directly. An alternative way is to solve the finite-time dynamics via a closed Lie algebra [18, 69] with the thermodynamic variables, the Hamiltonian  $H(t)$ , the Lagrange  $L(t) = \hat{p}^2/(2m) - m\omega(t)^2\hat{x}^2/2$  and the correlation function  $D(t) = \omega(t)(\hat{x}\hat{p} + \hat{p}\hat{x})/2$ . The closed differential equations of the expectations of the thermodynamic variables  $\langle H(t) \rangle = \text{Tr}[\rho(t)H(t)]$ ,  $\langle L(t) \rangle = \text{Tr}[\rho(t)L(t)]$  and  $\langle D(t) \rangle = \text{Tr}[\rho(t)D(t)]$  are obtained from Eq. (7) as

We exemplify the finite-time extrapolation method to obtain the thermodynamic length of the tuned harmonic oscillator through numerically solving the relaxation dynamics with the linear protocol  $\tilde{\omega}_{\text{li}}(s) = \omega_0 + (\omega_\tau - \omega_0)s$  and the optimal protocol  $\tilde{\omega}_{\text{op}}(s)$ . In the numerical calculation, the frequency is tuned from  $\omega_0 = 1$  to  $\omega_\tau = 2$  with the temperature  $k_B T_b = 1$  and the damping rate  $\kappa = 1$ . In Fig. 2, the extrapolated functions (curves) with  $N = 3$  are obtained from 10 sets of data (markers) with the duration  $\tau$  ranging from 6.4 to 9.9 for the linear (blue dashed line) and the optimal (the green solid line) protocols as  $\mathcal{L}_{\text{li}}(\tau) = 0.864 + 0.0128/\tau - 0.0464/\tau^2 - 0.145/\tau^3$  and  $\mathcal{L}_{\text{op}}(\tau) = 0.864 - 0.00471/\tau - 0.0448/\tau^2 - 0.168/\tau^3$ . The two extrapolated functions both give the consistent thermodynamic length identical to the theoretical result  $\mathcal{L} = 0.864$  by Eq. (10), as illustrated with the dotted black line. Therefore the current extrapolation method enables the measurement of the thermodynamic length in relatively short time without the need to find the optimal protocol.

The subset shows the  $\tau^{-1}$  scaling of the excess work. The black dotted line shows the bound  $\mathcal{L}^2/\tau$ , and the blue dashed (green solid) line shows the extra work with the linear (optimal) control scheme. The excess work of different protocols is indeed bounded by the thermodynamic length, and the bound is saturated by the optimal protocol.

*Compression of classical ideal gas.*— The extrapolation method is applicable in classical systems with the strategy shown in Fig. 1. We consider the finite-time compression of the classical ideal gas in a box, which is in contact with a heat bath at the temperature  $T_b$ . By compressing the piston, the volume of the box changes

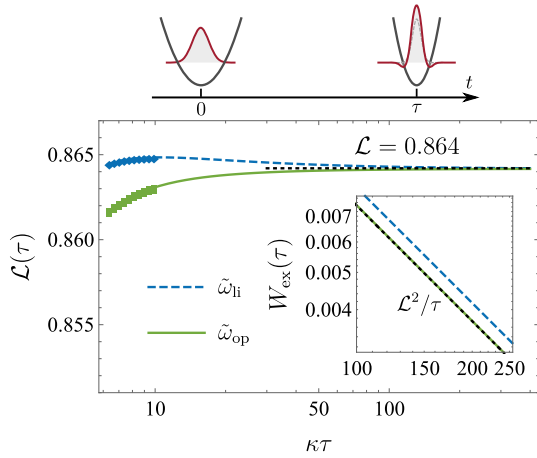


Figure 2. (Color online) Finite-time extrapolation to measure the thermodynamic length for the quantum Brownian motion in a tuned harmonic potential. The upper panel shows the frequency increases from  $\omega_0 = 1$  to  $\omega_\tau = 2$ . The temperature and the damping rate are set as  $k_B T_b = 1$  and  $\kappa = 1$ . In the lower panel, the black dotted line presents the thermodynamic length  $\mathcal{L} = 0.864$ , which is approached by the extrapolated functions with  $N = 3$  for both the linear (blue dashed curve) and the optimal (green solid curve) protocols. The subset shows the excess work in a slow process is bounded as  $W_{\text{ex}}(\tau) \geq \mathcal{L}^2/\tau$  (black dotted line), which is saturated by the optimal protocol at the long-time limit.

with the performed work rate  $\dot{W} = -p\dot{V}$ . With the state equation  $pV = nRT$ , the temperature  $T$  of the classical ideal gas satisfies

$$\frac{dT}{dt} = -\frac{nRT}{C_V} \frac{1}{V} \frac{dV}{dt} - \gamma(T - T_b), \quad (12)$$

where  $\gamma$  is the cooling rate in the Newton's law of cooling, assumed as a constant in the following discussion, and  $C_V$  is the heat capacity at the constant volume, e.g.  $C_V = 3nR/2$  for the single-atom ideal gas. In a finite-time isothermal process, the excess power is obtained as  $P_{\text{ex}}(t) = -nR(T - T_b)\dot{V}/V$ . The thermodynamic length  $\mathcal{L}$  is theoretically obtained as

$$\mathcal{L} = \sqrt{\frac{(nR)^2 T_b}{\gamma C_V} \left| \ln \frac{V_\tau}{V_0} \right|}. \quad (13)$$

For a long-time compression, the optimal protocol with the constant excess power is obtained as the exponential protocol  $\tilde{V}_{\text{op}}(s) = V_0(V_\tau/V_0)^s$ , which is consistent with the result obtained by the stochastic thermodynamics [38].

In Fig. 3, the finite-time thermodynamic lengths (markers) for given protocols are numerically obtained for the isothermal processes with the duration  $\tau$  ranging from 11.0 to 20.0, where the parameters are set as  $nR = T_b = \gamma = 1$  and  $C_V = 1.5$ , and the volume is tuned from  $V_0 = 1$  to  $V_\tau = 0.5$ . Two protocols are

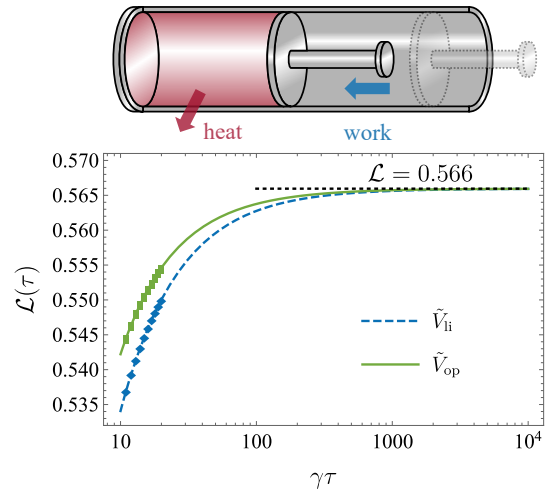


Figure 3. (Color online) Finite-time extrapolation to measure the thermodynamic length for the compression of the classical ideal gas in a box. The upper panel shows the compression of the box. In the lower panel, we use the linear protocol (blue dashed curve) and the optimal protocol (green solid curve) to compress the volume of the box to one half. With the current chosen parameters, the length extrapolated with the two protocols match the exact thermodynamic length  $\mathcal{L} = 0.566$  (black dotted line) by Eq. (13).

considered to tune the volume linearly  $\tilde{V}_{\text{li}}(s) = 1 - s/2$  (blue dashed curve) and exponentially  $\tilde{V}_{\text{op}}(s) = 2^{-s}$  (green solid curve). Setting the cutoff  $N = 3$ , the extrapolated functions of the two protocols are  $\mathcal{L}_{\text{li}}(\tau) = 0.566 - 0.318/\tau + 0.010/\tau^2 - 0.146/\tau^3$  and  $\mathcal{L}_{\text{op}}(\tau) = 0.566 - 0.216/\tau - 0.199/\tau^2 - 0.111/\tau^3$ . Both extrapolations with different protocols lead to the same value, matching the theoretical result  $\mathcal{L} = 0.566$  (black dotted line) given by Eq. (13).

Using examples of both the quantum harmonic oscillator and the classical ideal gas, we demonstrate the proposed extrapolation method for measuring the thermodynamic length for typical systems with single control parameter. The quantum harmonic oscillator system is potentially realized with the trapped ion [70, 71], and the classical ideal gas system will be tested with our recently designed apparatus [72].

*Conclusion.*—The thermodynamic length is crucial in optimization of finite-time isothermal processes, yet remains challenging to be practically measured in experiments. We have overcome the difficulty and proposed to measure the thermodynamic length via the finite-time extrapolation method, which allows to determine the lower bound of the excess work without necessarily using the optimal protocol. The protocol-independent property of the current measurement strategy benefits to practically measure the thermodynamic length in experiments. Based on our recent experimental setup [72], it is feasible to measure the thermodynamic length for the finite-time compression of the classical ideal gas in the experiments,



which we leave as the goal for our future experimental research.

Jin-Fu Chen thank Ruo-Xun Zhai for the helpful discussions about the dry-air experiment. This work is supported by the National Natural Science Foundation of China (NSFC) (Grants No. 11534002, No. 11875049, No. U1930402, and No. U1930403), and the National Basic Research Program of China (Grants No. 2016YFA0301201 and No. 2014CB921403).

---

\* cpsun@gcscaep.ac.cn

† hdong@gcscaep.ac.cn

- [1] R. S. Berry, V. A. Kazakov, S. Sieniutycz, Z. Szwast, and A. M. Tsvilin, *Thermodynamic Optimization of Finite-Time Processes* (John Wiley & Sons, Chichester, 2000).
- [2] M. de Koning, *J. Chem. Phys.* **122**, 104106 (2005).
- [3] T. Schmiedl and U. Seifert, *Phys. Rev. Lett.* **98**, 108301 (2007).
- [4] B. Andresen, *Angew. Chem. Int. Ed.* **50**, 2690 (2011).
- [5] V. Cavina, A. Mari, A. Carlini, and V. Giovannetti, *Phys. Rev. A* **98**, 052125 (2018).
- [6] A. P. Solon and J. M. Horowitz, *Phys. Rev. Lett.* **120**, 180605 (2018).
- [7] E. Aurell, C. Mejía-Monasterio, and P. Muratore-Ginanneschi, *Phys. Rev. Lett.* **106**, 250601 (2011).
- [8] E. Aurell, K. Gawędzki, C. Mejía-Monasterio, R. Mohayae, and P. Muratore-Ginanneschi, *J. Stat. Phys.* **147**, 487 (2012).
- [9] P. R. Zulkowski and M. R. DeWeese, *Phys. Rev. E* **89**, 052140 (2014).
- [10] K. Proesmans, J. Ehrich, and J. Bechhoefer, *Phys. Rev. Lett.* **125**, 100602 (2020).
- [11] K. Proesmans, J. Ehrich, and J. Bechhoefer, *Phys. Rev. E* **102**, 032105 (2020).
- [12] F. L. Curzon and B. Ahlborn, *Am. J. Phys.* **43**, 22 (1975).
- [13] M. Esposito, R. Kawai, K. Lindenberg, and C. V. den Broeck, *Phys. Rev. Lett.* **105**, 150603 (2010).
- [14] M. Esposito, R. Kawai, K. Lindenberg, and C. V. den Broeck, *Phys. Rev. E* **81**, 041106 (2010).
- [15] C. de Tomás, A. C. Hernández, and J. M. M. Roco, *Phys. Rev. E* **85**, 010104 (2012).
- [16] V. Cavina, A. Mari, A. Carlini, and V. Giovannetti, *Phys. Rev. A* **98**, 012139 (2018).
- [17] P. Abiuso and M. Perarnau-Llobet, *Phys. Rev. Lett.* **124**, 110606 (2020).
- [18] S. Lee, M. Ha, J.-M. Park, and H. Jeong, *Phys. Rev. E* **101**, 022127 (2020).
- [19] S. Singh, *Int. J. Theor. Phys.* **59**, 2889 (2020).
- [20] Y. Zhang, *J. Stat. Phys.* **178**, 1336 (2020).
- [21] F. Weinhold, *J. Chem. Phys.* **63**, 2479 (1975).
- [22] G. Ruppeiner, *Phys. Rev. A* **20**, 1608 (1979).
- [23] R. Gilmore, *Phys. Rev. A* **30**, 1994 (1984).
- [24] P. Salamon, J. D. Nulton, and R. S. Berry, *J. Chem. Phys.* **82**, 2433 (1985).
- [25] G. Ruppeiner, *Rev. Mod. Phys.* **67**, 605 (1995).
- [26] G. E. Crooks, *Phys. Rev. Lett.* **99**, 100602 (2007).
- [27] E. H. Feng and G. E. Crooks, *Phys. Rev. E* **79**, 012104 (2009).
- [28] P. Salamon, A. Nitzan, B. Andresen, and R. S. Berry, *Phys. Rev. A* **21**, 2115 (1980).
- [29] L. Diósi, K. Kulacsy, B. Lukács, and A. Rácz, *J. Chem. Phys.* **105**, 11220 (1996).
- [30] P. R. Zulkowski and M. R. DeWeese, *Phys. Rev. E* **92**, 032113 (2015).
- [31] P. R. Zulkowski and M. R. DeWeese, *Phys. Rev. E* **92**, 032117 (2015).
- [32] M. V. S. Bonança and S. Deffner, *J. Chem. Phys.* **140**, 244119 (2014).
- [33] M. V. S. Bonança and S. Deffner, *Phys. Rev. E* **98**, 042103 (2018).
- [34] Y. Zhang, *Europhys. Lett.* **128**, 30002 (2020).
- [35] P. Salamon and R. S. Berry, *Phys. Rev. Lett.* **51**, 1127 (1983).
- [36] J. Nulton, P. Salamon, B. Andresen, and Q. Anmin, *J. Chem. Phys.* **83**, 334 (1985).
- [37] Z.-C. Tu, *Chin. Phys. B* **21**, 020513 (2012).
- [38] Z. Gong, Y. Lan, and H. Quan, *Phys. Rev. Lett.* **117**, 180603 (2016).
- [39] V. Cavina, A. Mari, and V. Giovannetti, *Phys. Rev. Lett.* **119**, 050601 (2017).
- [40] Y.-H. Ma, D. Xu, H. Dong, and C.-P. Sun, *Phys. Rev. E* **98**, 042112 (2018).
- [41] D. A. Sivak and G. E. Crooks, *Phys. Rev. Lett.* **108**, 190602 (2012).
- [42] P. R. Zulkowski, D. A. Sivak, G. E. Crooks, and M. R. DeWeese, *Phys. Rev. E* **86**, 041148 (2012).
- [43] G. M. Rotskoff and G. E. Crooks, *Phys. Rev. E* **92**, 060102 (2015).
- [44] D. A. Sivak and G. E. Crooks, *Phys. Rev. E* **94**, 052106 (2016).
- [45] M. Esposito, U. Harbola, and S. Mukamel, *Rev. Mod. Phys.* **81**, 1665 (2009).
- [46] M. Campisi, P. Hänggi, and P. Talkner, *Rev. Mod. Phys.* **83**, 771 (2011).
- [47] R. Kosloff, *Entropy* **15**, 2100 (2013).
- [48] S. Vinjanampathy and J. Anders, *Contemp. Phys.* **57**, 545 (2016).
- [49] P. Strasberg, G. Schaller, T. Brandes, and M. Esposito, *Phys. Rev. X* **7**, 021003 (2017).
- [50] S. Deffner and E. Lutz, *Phys. Rev. Lett.* **105**, 170402 (2010).
- [51] S. Deffner and E. Lutz, *Phys. Rev. E* **87**, 022143 (2013).
- [52] L. Mancino, V. Cavina, A. D. Pasquale, M. Sbroscia, R. I. Booth, E. Roccia, I. Gianani, V. Giovannetti, and M. Barbieri, *Phys. Rev. Lett.* **121**, 160602 (2018).
- [53] D. P. Pires, M. Cianciaruso, L. C. Céleri, G. Adesso, and D. O. Soares-Pinto, *Phys. Rev. X* **6**, 021031 (2016).
- [54] I. Bengtsson, *Geometry of Quantum States* (Cambridge University Press, Cambridge, 2017).
- [55] M. Scandi and M. Perarnau-Llobet, *Quantum* **3**, 197 (2019).
- [56] K. Brandner and K. Saito, *Phys. Rev. Lett.* **124**, 040602 (2020).
- [57] P. Abiuso, H. J. D. Miller, M. Perarnau-Llobet, and M. Scandi, *Entropy* **22**, 1076 (2020).
- [58] H. J. Miller and M. Mehboudi, *Phys. Rev. Lett.* **125**, 260602 (2020).
- [59] T. Albash, S. Boixo, D. A. Lidar, and P. Zanardi, *New J. Phys.* **14**, 123016 (2012).
- [60] M. Yamaguchi, T. Yuge, and T. Ogawa, *Phys. Rev. E* **95**, 012136 (2017).
- [61] R. Dann, A. Levy, and R. Kosloff, *Phys. Rev. A* **98**, 052129 (2018).

- [62] R. Alicki, *J. Phys. A: Math. Gen.* **12**, L103 (1979).
- [63] D. Mandal and C. Jarzynski, *J. Stat. Mech: Theory Exp.* **2016**, 063204 (2016).
- [64] G. E. Crooks, “On the drazin inverse of the rate matrix,” (2018).
- [65] Supplementary materials.
- [66] C. Jarzynski, *Phys. Rev. Lett.* **78**, 2690 (1997).
- [67] A. Caldeira and A. Leggett, *Physica A* **121**, 587 (1983).
- [68] H.-P. Breuer and F. Petruccione, *The Theory of Open Quantum Systems* (Oxford University Press, 2007).
- [69] Y. Rezek and R. Kosloff, *New J. Phys.* **8**, 83 (2006).
- [70] S. An, M. Um, D. Lv, Y. Lu, J. Zhang, H. Quan, Z. Yin, J. N. Zhang, and K. Kim, *Nat. Phys.* **11**, 193 (2014).
- [71] J. Rosnagel, S. T. Dawkins, K. N. Tolazzi, O. Abah, E. Lutz, F. Schmidt-Kaler, and K. Singer, *Science* **352**, 325 (2016).
- [72] Y.-H. Ma, R.-X. Zhai, J. Chen, C. Sun, and H. Dong, *Phys. Rev. Lett.* **125**, 210601 (2020).

# Supplementary Materials: Extrapolating the thermodynamic length with finite-time measurements

Jin-Fu Chen,<sup>1,2</sup> Chang-Pu Sun,<sup>1,2,\*</sup> and Hui Dong<sup>2,†</sup>

<sup>1</sup>*Beijing Computational Science Research Center, Beijing 100193, China*

<sup>2</sup>*Graduate School of China Academy of Engineering Physics,*

*No. 10 Xibeiwang East Road, Haidian District, Beijing, 100193, China*

(Dated: June 19, 2021)

The document is devoted to providing detailed derivations and supporting discussions to the main content. In Sec. **I**, we show the convergence of the finite-time thermodynamic length to the thermodynamic length with the increasing process time  $\tau$ . In Sec. **II**, we show the example of the tuned two-level system, and optimize the protocol with the Drazin inverse of the Lindblad operator. In Sec. **III**, we show detailed discussions for the tuned harmonic oscillator, especially the derivation of Eq. (8) in the main content. In Sec. **IV**, we consider the thermodynamic length for the pedagogical model of the classical ideal gas system, which was used to validate the  $\tau^{-1}$  scaling of the excess work in our recent experiment [1].

## I. CONVERGENCE OF THE FINITE-TIME THERMODYNAMIC LENGTH

We demonstrate the convergence of the finite-time thermodynamic length  $\mathcal{L} = \lim_{\tau \rightarrow \infty} \mathcal{L}(\tau)$ . Plugging into the series expansion of the excess power by Eq. (5) in the main content, the finite-time thermodynamic length is rewritten as

$$\mathcal{L}(\tau) = \int_0^1 \sqrt{\sum_{n=1}^{\infty} \text{Tr}\left\{\frac{\partial \tilde{H}(s)}{\partial s} \tau^{1-n} (\mathcal{L}_{\tilde{\lambda}(s)}^{-1} \frac{\partial}{\partial s})^n [\tilde{\rho}_{\text{eq}}(s)]\right\}} ds. \quad (1)$$

With the increasing control time  $\tau$ , the term with  $n = 1$  is independent of  $\tau$  and dominates the summation, and leads to the thermodynamic length

$$\mathcal{L} = \int_0^1 \sqrt{\text{Tr}\left\{\frac{\partial \tilde{H}(s)}{\partial s} (\mathcal{L}_{\tilde{\lambda}(s)}^{-1} \frac{\partial}{\partial s}) [\tilde{\rho}_{\text{eq}}(s)]\right\}} ds, \quad (2)$$

$$= \int_0^1 \sqrt{[\tilde{\lambda}'(s)]^2 \text{Tr}\left[\left(\frac{\partial H}{\partial \lambda}\right) \left(\mathcal{L}_{\tilde{\lambda}(s)}^{-1} \frac{\partial \tilde{\rho}_{\text{eq}}}{\partial \lambda}\right)\right]} ds, \quad (3)$$

$$= \int_{\lambda_0}^{\lambda_1} \sqrt{\text{Tr}\left(\frac{\partial H}{\partial \lambda}\right) \left(\mathcal{L}_{\lambda}^{-1} \frac{\partial \rho_{\text{eq}}}{\partial \lambda}\right) |d\lambda|}. \quad (4)$$

The last integral shows  $\mathcal{L}$  is independent of the protocol  $\tilde{\lambda}(s)$  for tuning a single control parameter.

## II. TWO-LEVEL SYSTEM WITH TUNED ENERGY SPACING

In this section, we show the example of two-level system with tuned energy spacing. The Drazin Inverse of the Lindblad operator is obtained directly for the optimization of the protocol. The system Hamiltonian of the two-level system reads

$$H(t) = \frac{E(t)}{2} (|e\rangle \langle e| - |g\rangle \langle g|), \quad (5)$$

where the energy spacing  $E(t)$  is the control parameter. The state of the two-level system is represented with the density matrix

$$\rho(t) = \begin{pmatrix} \rho_{ee} & \rho_{eg} \\ \rho_{ge} & \rho_{gg} \end{pmatrix}. \quad (6)$$

With the coupling to the heat bath, the evolution is governed by the time-dependent master equation

$$\dot{\rho} = \mathcal{L}_{E(t)}(\rho), \quad (7)$$

where  $\mathcal{L}_{E(t)}$  is in the Lindblad form

$$\mathcal{L}_{E(t)}(\rho) = -i[H(t), \rho] + \gamma_{\uparrow}(t)\mathcal{D}(\sigma_{+})[\rho] + \gamma_{\downarrow}(t)\mathcal{D}(\sigma_{-})[\rho], \quad (8)$$

with the transition operators  $\sigma_{+} = |e\rangle\langle g|$ ,  $\sigma_{-} = |g\rangle\langle e|$  and the dissipation super-operator

$$\mathcal{D}(\sigma)[\rho] = \sigma\rho\sigma^{\dagger} - \frac{1}{2}\sigma^{\dagger}\sigma\rho - \frac{1}{2}\rho\sigma^{\dagger}\sigma. \quad (9)$$

The time-dependent transition rates are  $\gamma_{\uparrow}(t) = \gamma(t)N(t)$  and  $\gamma_{\downarrow}(t) = \gamma(t)[N(t) + 1]$  with the average phonon number

$$N(t) = \frac{1}{e^{\beta_b E(t)} - 1}, \quad (10)$$

The spontaneous emission rate  $\gamma(t)$  relies on the bath spectral as

$$\gamma(t) = \gamma_0 E(t)^{\alpha}. \quad (11)$$

Equation (8) extends the well-known Lindblad master equation [2] for the tuned two-level system via the time-dependent energy spacing  $E(t)$ . This approximation is suitable for a long-time isothermal process with slowly tuned control parameters.

Rewriting the density matrix into a vector

$$\rho = \begin{pmatrix} \rho_{ee} & \rho_{gg} & \rho_{eg} & \rho_{ge} \end{pmatrix}^{\text{T}}, \quad (12)$$

the Lindblad operator is presented in the matrix form as

$$\mathcal{L}_{E(t)} = \begin{pmatrix} -\gamma(N+1) & \gamma N & 0 & 0 \\ \gamma(N+1) & -\gamma N & 0 & 0 \\ 0 & 0 & -\gamma(N+\frac{1}{2}) - iE & 0 \\ 0 & 0 & 0 & -\gamma(N+\frac{1}{2}) + iE \end{pmatrix}, \quad (13)$$

with the eigenvalues  $\Gamma = 0, -\gamma(N+1/2) \pm iE$ , and  $\gamma(2N+1)$ . The Drazin inverse of the Lindblad operator is obtained as

$$\mathcal{L}_{E(t)}^{-1} = \begin{pmatrix} -\frac{(N+1)}{\gamma(2N+1)^2} & \frac{N}{\gamma(2N+1)^2} & 0 & 0 \\ \frac{(N+1)}{\gamma(2N+1)^2} & -\frac{N}{\gamma(2N+1)^2} & 0 & 0 \\ 0 & 0 & \frac{1}{-\gamma(N+\frac{1}{2})-iE} & 0 \\ 0 & 0 & 0 & \frac{1}{-\gamma(N+\frac{1}{2})+iE} \end{pmatrix}. \quad (14)$$

At the time  $t$ , the instantaneous equilibrium state is

$$\rho_{\text{eq}}(t) = \begin{pmatrix} \frac{N(t)}{2N(t)+1} & \frac{N(t)+1}{2N(t)+1} & 0 & 0 \end{pmatrix}^{\text{T}}. \quad (15)$$

The off-diagonal terms of the density matrix remain zero  $\rho_{\text{eg}}(t) = \rho_{\text{ge}}^*(t) = 0$  during the whole isothermal process. The excess power to the first order is



$$P_{\text{ex}}^{[1]}(t) = \text{Tr}\left[\frac{dH(t)}{dt} \mathcal{L}_{E(t)}^{-1}\left(\frac{d\rho_{\text{eq}}(t)}{dt}\right)\right] \quad (16)$$

$$= \frac{\beta_b \dot{E}^2 \tanh\left(\frac{1}{2}\beta_b E\right)}{4\gamma \cosh^2\left(\frac{1}{2}\beta_b E\right)}. \quad (17)$$

The thermodynamic length follows as

$$\mathcal{L} = \int_{E_0}^{E_\tau} \sqrt{\frac{\beta_b \tanh\left(\frac{1}{2}\beta_b E(t)\right)}{4\gamma_0 E^\alpha \cosh^2\left(\frac{1}{2}\beta_b E(t)\right)}} dE. \quad (18)$$

At the long-time limit, the optimal protocol  $\tilde{E}(s)$  is obtained with the constant excess power  $P_{\text{ex}}^{[1]}(t) = \text{const}$ , namely

$$\frac{\beta_b \tanh\left(\frac{1}{2}\beta_b \tilde{E}(s)\right)}{4\gamma_0 \tilde{E}(s)^\alpha \cosh^2\left(\frac{1}{2}\beta_b \tilde{E}(s)\right)} \left(\frac{d\tilde{E}(s)}{ds}\right)^2 = \text{const}. \quad (19)$$

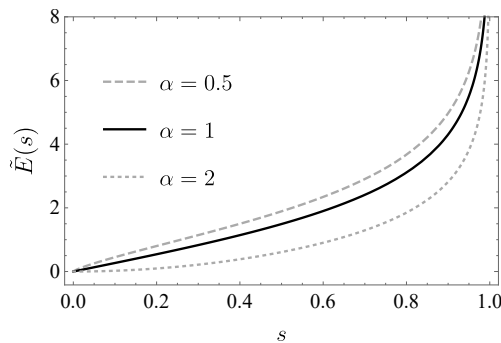


Figure 1. The optimal protocols of tuning the energy spacing  $\tilde{E}(s)$  of the two-level system with different bath spectral  $\alpha = 0.5, 1$  and  $2$ . The optimal protocols are obtained by numerically solving Eq. (19) with the parameters  $\beta_b = 1$  and  $\gamma_0 = 1$ .

Figure 1 shows the tuning of the energy spacing  $\tilde{E}(s)$  with  $s$  ranging from  $0$  to  $1$ . We solve the optimal protocols for different bath spectral, the sub-Ohmic  $\alpha = 0.5$  (the dashed curve), the Ohmic  $\alpha = 1$  (the dotted curve), and super-Ohmic  $\alpha = 2$  (the dash-dotted curve) with the inverse temperature  $\beta_b = 1$  and the dissipation strength  $\gamma_0 = 1$ .

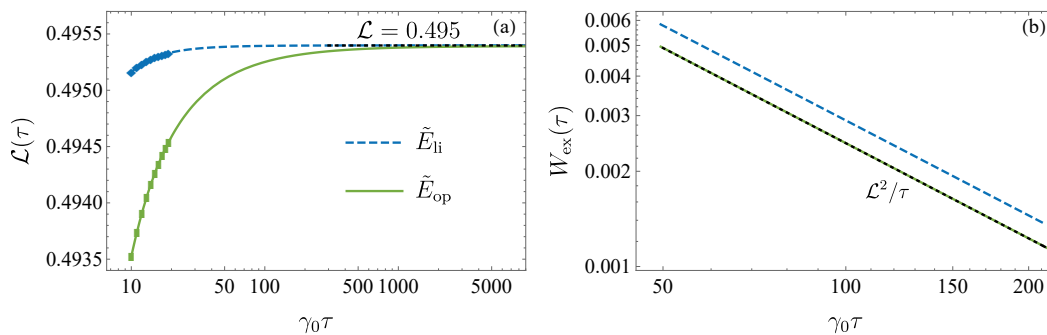


Figure 2. Finite-time extrapolation for the two-level system with the tuned energy spacing. (a) Finite-time thermodynamic lengths for the linear and the optimal protocols. Through measuring the finite-time thermodynamic length with short duration (markers), the thermodynamic length can be approached by the extrapolated functions of both protocols. (b) The  $\tau^{-1}$  scaling of the excess work. For a long-time process, the optimal protocol (green solid line) consumes less excess work, and saturates the lower bound given by the thermodynamic length (black dotted line).

With the Ohmic spectral  $\alpha = 1$  of the bath, we exemplify the extrapolation method to measure the thermodynamic length of the two-level system. The energy spacing is tuned from  $E_0 = 1$  to  $E_\tau = 2$  with the linear and the optimal

protocols. Figure 2(a) shows the measured finite-time thermodynamic length  $\mathcal{L}(\tau) = \int_0^\tau \sqrt{P_{\text{ex}}(t)} dt$  (markers) with the duration ranging from 10.0 to 19.0. With the cutoff  $N = 3$ , the extrapolated functions are obtained for the two protocols as  $\mathcal{L}_{\text{li}}(\tau) = 0.495 - 0.000284/\tau - 0.0179/\tau^2 - 0.0307/\tau^3$  and  $\mathcal{L}_{\text{op}}(\tau) = 0.495 - 0.0136/\tau - 0.0500/\tau^2 - 0.0130/\tau^3$ . They both approach the thermodynamic length (black dotted line) with the increasing duration  $\tau$ . Figure 2(b) shows the  $\tau^{-1}$  scaling of the excess work at the long-time limit. The excess work is bounded by the thermodynamic length as  $W_{\text{ex}} \geq \mathcal{L}^2/\tau$ . The excess work done with the optimal protocol matches the lower bound given by the thermodynamic length (black dotted line).

### III. QUANTUM BROWNIAN MOTION IN A TUNED HARMONIC POTENTIAL

#### A. Differential equations of the average values

We first derive the differential equations of the average values of the internal energy  $\langle H(t) \rangle = \text{Tr}[\rho(t)H(t)]$ , the Lagrange  $\langle L(t) \rangle = \text{Tr}[\rho(t)L(t)]$  and the correlation function  $\langle D(t) \rangle = \text{Tr}[\rho(t)D(t)]$  in the main content. According to the Caldeira-Leggett master equation [2, 3], the time derivative of the internal energy is calculated as

$$\frac{d}{dt} \langle H \rangle = m\omega(t)\dot{\omega}(t)\text{Tr}[\rho(t)\hat{x}^2] + \text{Tr}\{\mathcal{L}_{\omega(t)}[\rho(t)]H(t)\}, \quad (20)$$

where the upper dot denotes the time derivative, namely  $\dot{\omega}(t) = d\omega/dt$ . With the similar calculation of time derivatives for the Lagrange and the correlation function, we obtain the evolution of average values as

$$\frac{d}{dt} \langle H \rangle = \frac{\dot{\omega}}{\omega} (\langle H \rangle - \langle L \rangle) - 2\kappa(\langle H \rangle + \langle L \rangle) + 2\kappa k_B T_b, \quad (21)$$

$$\frac{d}{dt} \langle L \rangle = -\frac{\dot{\omega}}{\omega} (\langle H \rangle - \langle L \rangle) - 2\omega \langle D \rangle - 2\kappa(\langle H \rangle + \langle L \rangle) + 2\kappa k_B T_b, \quad (22)$$

$$\frac{d}{dt} \langle D \rangle = \frac{\dot{\omega}}{\omega} \langle D \rangle + 2\omega \langle L \rangle - 2\kappa \langle D \rangle, \quad (23)$$

The three equations above are Eqs. (8) in the main context.

Let us rewrite these differential equations into a compact form

$$\frac{d}{dt} \phi = M(t)\phi + f(t), \quad (24)$$

with the vector  $\phi = (\langle H \rangle \ \langle L \rangle \ \langle D \rangle)^T$  and the function  $f(t) = 2\kappa k_B T_b (1 \ 1 \ 0)^T$ . The matrix  $M(t)$  is

$$M(t) = \begin{pmatrix} -2\kappa + \frac{\dot{\omega}}{\omega} & -2\kappa - \frac{\dot{\omega}}{\omega} & 0 \\ -2\kappa - \frac{\dot{\omega}}{\omega} & -2\kappa + \frac{\dot{\omega}}{\omega} & -2\omega \\ 0 & 2\omega & -2\kappa + \frac{\dot{\omega}}{\omega} \end{pmatrix}, \quad (25)$$

the inverse of which is obtained as

$$M^{-1} = \begin{pmatrix} -\frac{(\frac{\dot{\omega}}{\omega} - 2\kappa)^2 + 4\omega^2}{4(\frac{\dot{\omega}}{\omega} - 2\kappa)(2\kappa\frac{\dot{\omega}}{\omega} - \omega^2)} & \frac{\frac{\dot{\omega}}{\omega} + 2\kappa}{4(\omega^2 - 2\kappa\frac{\dot{\omega}}{\omega})} & \frac{\omega(\frac{\dot{\omega}}{\omega} + 2\kappa)}{2(\frac{\dot{\omega}}{\omega} - 2\kappa)(\omega^2 - 2\kappa\frac{\dot{\omega}}{\omega})} \\ \frac{\frac{\dot{\omega}}{\omega} + 2\kappa}{4(\omega^2 - 2\kappa\frac{\dot{\omega}}{\omega})} & \frac{2\kappa - \frac{\dot{\omega}}{\omega}}{4(2\kappa\frac{\dot{\omega}}{\omega} - \omega^2)} & \frac{\omega}{2(\omega^2 - 2\kappa\frac{\dot{\omega}}{\omega})} \\ \frac{\omega(\frac{\dot{\omega}}{\omega} + 2\kappa)}{2(\frac{\dot{\omega}}{\omega} - 2\kappa)(2\kappa\frac{\dot{\omega}}{\omega} - \omega^2)} & \frac{\omega}{2(2\kappa\frac{\dot{\omega}}{\omega} - \omega^2)} & \frac{\gamma\frac{\dot{\omega}}{\omega}}{4(\frac{\dot{\omega}}{\omega} - 2\kappa)(2\kappa\frac{\dot{\omega}}{\omega} - \omega^2)} \end{pmatrix}. \quad (26)$$

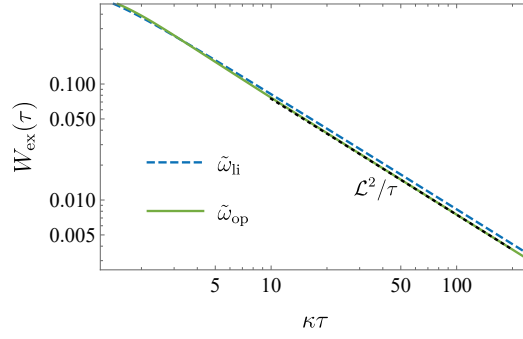


Figure 3.  $\tau^{-1}$  scaling of the excess work for tuning the frequency of the harmonic oscillator. We compare the excess work in the linear protocol (blue dashed curve) and the optimal protocol (green solid curve). The frequency is tuned from  $\omega_0 = 1$  to  $\omega_\tau = 2$  with the temperature  $k_B T_b = 1$ , and the dissipation rate is set as  $\kappa = 1$ . For the slow process, the lower bound of the excess work  $\mathcal{L}^2/\tau$  is given by the thermodynamic length with  $\mathcal{L} = 0.864$ .

## B. Solution of slow tuning

With the existence of the inverse  $M^{-1}$ , we rewrite the differential equation as

$$\phi = -M^{-1}f + M^{-1}\frac{d}{dt}\phi. \quad (27)$$

Using the perturbative expansion approach in Ref. [4], the solution for the slow tuning is

$$\phi = -\sum_{n=0}^{\infty} (M^{-1}\frac{d}{dt})^n M^{-1}f, \quad (28)$$

where the time derivative  $d/dt$  acts on both  $M^{-1}$  and  $f$ . For the slow tuning satisfied

$$\frac{\dot{\omega}}{\kappa\omega} \ll 1, \quad \frac{\kappa\dot{\omega}}{\omega^3} \ll 1, \quad (29)$$

the term with  $n = 0$  dominates the summation in Eq. (28), namely

$$\phi \approx -M^{-1}f = k_B T_b \begin{pmatrix} \frac{\kappa[2\omega^2 + \frac{\dot{\omega}}{\omega}(\frac{\dot{\omega}}{\omega} - 2\kappa)]}{(2\kappa - \frac{\dot{\omega}}{\omega})(\omega^2 - 2\kappa\frac{\dot{\omega}}{\omega})} \\ \frac{\kappa\dot{\omega}}{2\kappa\dot{\omega} - \omega^3} \\ -\frac{\frac{\dot{\omega}}{\omega^2}}{(2\kappa - \frac{\dot{\omega}}{\omega})(\omega^2 - 2\kappa\frac{\dot{\omega}}{\omega})} \end{pmatrix}. \quad (30)$$

Keeping the first order of  $\dot{\omega}/(\kappa\omega)$ ,  $\kappa\dot{\omega}/\omega^3$  and  $\dot{\omega}/\omega^2$ , we obtain

$$\phi^{[1]} \approx k_B T_b \begin{pmatrix} 1 + \kappa\frac{\dot{\omega}}{\omega^3} + \frac{1}{2\kappa}\frac{\dot{\omega}}{\omega} \\ -\kappa\frac{\dot{\omega}}{\omega^3} \\ -\frac{\dot{\omega}}{\omega^2} \end{pmatrix}. \quad (31)$$

The terms with the change of the frequency  $\dot{\omega}$  contributes to the  $\tau^{-1}$  scaling of the excess work at the long-time limit.

The power for tuning the frequency is

$$\dot{W}(t) = \frac{\dot{\omega}}{\omega} (\langle H \rangle - \langle L \rangle), \quad (32)$$

and the quasi-static work rate is  $\dot{W}_{(0)}(t) = k_B T_b \dot{\omega}/\omega$ . Plugging Eq. (31) into the power, we obtain the excess power  $P_{\text{ex}}(t) = \dot{W}(t) - \dot{W}_{(0)}(t)$  to the lowest order of  $\dot{\omega}$  as

$$P_{\text{ex}}(t) \approx k_B T_b \frac{\dot{\omega}^2}{\omega^2} \left( \frac{1}{2\kappa} + \frac{2\kappa}{\omega^2} \right), \quad (33)$$

which leads to the thermodynamic length

$$\mathcal{L} = \int_{\omega_0}^{\omega_\tau} \sqrt{k_B T_b \left( \frac{1}{2\kappa} + \frac{2\kappa}{\omega^2} \right) \left| \frac{d\omega}{\omega} \right|}. \quad (34)$$

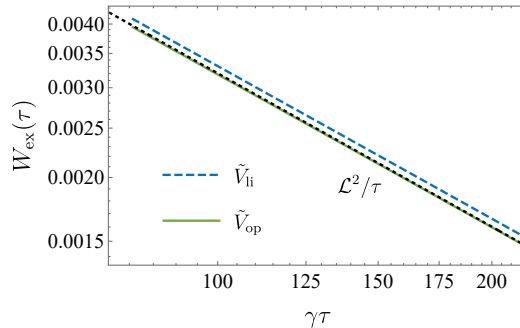


Figure 4.  $\tau^{-1}$  scaling of the excess work for the finite-time compression of the ideal gas. The linear protocol  $\tilde{V}_{\text{li}}(s) = V_0 + (V_\tau - V_0)s$  and the exponential protocol  $\tilde{V}_{\text{op}}(s) = V_0(V_\tau/V_0)^s$  are considered. The parameters are set as  $nR = T_b = \gamma = 1$  and  $C_V = 1.5$  with the volume tuned from  $V_0 = 1$  to  $V_\tau = 0.5$ . The black dotted line shows the lower bound of the excess work  $W_{\text{ex}} \geq \mathcal{L}^2/\tau$  given by the thermodynamic length  $\mathcal{L} = 0.566$ , saturated by the exponential protocol.

### C. Numerical result of the excess work

In Fig. 3, we show the numerical result of the excess work corresponding to the subset of Fig. 2 in the main content. We consider the linear protocol (blue dashed curve) with  $\tilde{\omega}_{\text{li}}(s) = \omega_0 + (\omega_\tau - \omega_0)s$  and the optimal protocol (green solid curve) with  $\tilde{\omega}_{\text{op}}(s)$  solved by Eq. (10) in the main content. For the slow tuning with long duration, the excess work satisfies the  $\tau^{-1}$  scaling, and is bounded by the thermodynamic length as  $W_{\text{ex}} \geq \mathcal{L}^2/\tau$ . The lower bound (black dotted line) is saturated by the optimal protocol.

## IV. COMPRESSION OF CLASSICAL IDEAL GAS

Our recent experimental setup for validation of the  $\tau^{-1}$  scaling of the excess work with the ideal gas [1] can be used to apply the current strategy to measure the thermodynamic length. Here we show the theoretical derivation of the thermodynamic length and the excess work for the finite-time compression.

Defining the temperature difference  $u = T - T_b$ , we rewrite Eq. (11) in the main content as

$$\frac{du}{dt} = -\frac{nR}{C_V}(T_b + u)\frac{\dot{V}}{V} - \gamma u. \quad (35)$$

The series expansion solution is obtained as

$$u = \sum_{n=0}^{\infty} \left( -\frac{1}{\frac{nR}{C_V}\frac{\dot{V}}{V} + \gamma} \frac{d}{dt} \right)^n \left( \frac{-\frac{nRT_b}{C_V}\frac{\dot{V}}{V}}{\frac{nR}{C_V}\frac{\dot{V}}{V} + \gamma} \right). \quad (36)$$

The power of the compression is  $\dot{W} = -p\dot{V} = -nRT\dot{V}/V$ . In the quasi-static process, the temperature of the gas is the same as that of the bath, i.e.  $T = T_b$ , and the quasi-static work rate is  $\dot{W}_{(0)}(t) = -nRT_b\dot{V}/V$ . For the slow tuning  $(nR/\gamma C_V)(\dot{V}/V) \ll 1$ , the term with  $n = 0$  dominates the summation in Eq. (36), and the temperature difference to the lowest order is  $u^{[1]} = -(nRT_b/\gamma C_V)(\dot{V}/V)$ . The excess power  $P_{\text{ex}} = \dot{W} - \dot{W}_{(0)}(t)$  approximates

$$P_{\text{ex}} \approx \frac{(nR)^2 T_b}{\gamma C_V} \left( \frac{\dot{V}}{V} \right)^2, \quad (37)$$

with the excess work

$$W_{\text{ex}} \approx \int_0^\tau \frac{(nR)^2 T_b}{\gamma C_V} \left( \frac{\dot{V}}{V} \right)^2 dt. \quad (38)$$

The thermodynamic length follows as

$$\mathcal{L} = \int_0^\tau \sqrt{\frac{(nR)^2 T_b}{\gamma C_V} \left(\frac{\dot{V}}{V}\right)^2} dt, \quad (39)$$

which gives Eq. (12) in the main content.

In Fig. 4, we show the numerical result of the excess work for the finite-time compression of ideal gas. The excess work exhibits the  $\tau^{-1}$  scaling during the slow compression process. The compression with the exponential protocol (green solid curve) consumes the lower excess work compared to that of the linear protocol (blue dashed curve) with given duration  $\tau$ . The lower bound  $\mathcal{L}^2/\tau$  (black dotted line) is saturated by the optimal protocol as the exponential protocol.

---

\* [cpsun@gscaep.ac.cn](mailto:cpsun@gscaep.ac.cn)

† [hdong@gscaep.ac.cn](mailto:hdong@gscaep.ac.cn)

- [1] Y.-H. Ma, R.-X. Zhai, J. Chen, C. Sun, and H. Dong, *Phys. Rev. Lett.* **125**, 210601 (2020).
- [2] H.-P. Breuer and F. Petruccione, *The Theory of Open Quantum Systems* (Oxford University Press, 2007).
- [3] A. Caldeira and A. Leggett, *Physica A* **121**, 587 (1983).
- [4] V. Cavina, A. Mari, and V. Giovannetti, *Phys. Rev. Lett.* **119**, 050601 (2017).